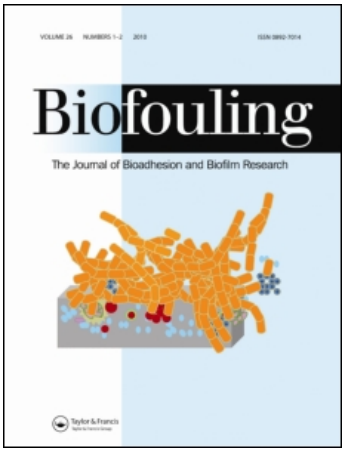

Biofouling
Publication details, including instructions for authors and subscription information:
http://www.informaworld.com/smpp/title~content=t713454511

Biofilm formation at warming temperature: acceleration of microbial colonization and microbial interactive effects

Verónica Díaz Villanueva[a]; Jordi Font[b]; Thomas Schwartz[c]; Anna M. Romaní[b]
[a] Lab. Limnología,INIBIOMA-CONICET, Bariloche, Argentina [b] Institute of Aquatic Ecology, Department of Environmental Sciences, University of Girona, Girona, Spain [c] Department of Microbiology of Natural and Technical Interfaces, Karlsruhe Institute of Technology, Institute of Functional Interfaces, Karlsruhe, Germany

First published on: 28 November 2010

To cite this Article Villanueva, Verónica Díaz , Font, Jordi , Schwartz, Thomas and Romaní, Anna M.(2011) 'Biofilm formation at warming temperature: acceleration of microbial colonization and microbial interactive effects', Biofouling, 27: 1, 59 — 71, First published on: 28 November 2010 (iFirst)
To link to this Article: DOI: 10.1080/08927014.2010.538841
URL: http://dx.doi.org/10.1080/08927014.2010.538841

Biofouling
Vol. 27, No. 1, January 2011, 59–71

Taylor & Francis
Taylor & Francis Group

Biofilm formation at warming temperature: acceleration of microbial colonization and microbial interactive effects

Verónica Díaz Villanueva[a]*, Jordi Font[b], Thomas Schwartz[c] and Anna M. Romaní[b]

[a]*Lab. Limnología,INIBIOMA-CONICET, Bariloche, Argentina;* [b]*Institute of Aquatic Ecology, Department of Environmental Sciences, University of Girona, Girona, Spain;* [c]*Karlsruhe Institute of Technology, Institute of Functional Interfaces, Department of Microbiology of Natural and Technical Interfaces, Karlsruhe, Germany*

(*Received 30 August 2010; final version received 4 November 2010*)

River biofilms that grow on wet benthic surface are mainly composed of bacteria, algae, cyanobacteria and protozoa embedded in a polysaccharide matrix. The effects of increased river water temperature on biofilm formation were investigated. A laboratory experiment was designed employing two temperatures (11.1–13.2°C, night–day; 14.7–16.0°C, night–day) and two nutrient levels (0.054 mg P l^{-1}, 0.75 mg N l^{-1}; 0.54 mg P l^{-1}, 7.5 mg N l^{-1}). Biofilm formation at the higher temperature was faster, while the biomass of the mature biofilm was mainly determined by nutrient availability. The specific response of the three microbial groups that colonized the substrata (algae, bacteria and ciliates) was modulated by interactions between them. The greater bacterial growth rate and earlier bacterial colonization at the higher temperature and higher nutrient status was not translated into the accrual of higher bacterial biomass. This may result from ciliates grazing on the bacteria, as shown by an earlier increase in peritrichia at higher temperatures, and especially at high nutrient conditions. Temperature and ciliate grazing might determine the growth of a distinctive bacterial community under warming conditions. Warmer conditions also produced a thicker biofilm, while functional responses were much less evident (increases in the heterotrophic utilization of polysaccharides and peptides, but no increase in primary production and respiration). Increasing the temperature of river water might lead to faster biofilm recolonization after disturbances, with a distinct biofilm community structure that might affect the trophic web. Warming effects would be expected to be more relevant under eutrophic conditions.

Keywords: biofilm; temperature; nutrient; algae; bacteria; ciliate; extracellular enzymes

Introduction

Freshwater biofilms can grow on any wet benthic surface (cobbles, sand, leaves and wood) and are mainly composed of bacteria, algae, cyanobacteria, fungi and protozoa embedded in a polymeric matrix (Lock 1993). Because of their autotrophic and heterotrophic metabolism, biofilm communities are major sites for the uptake, storage and transformation of fluvial dissolved organic matter and nutrients and play a major role in stream metabolism (Romaní et al. 2004; Bott et al. 2006). Biofilms are fast-growing microbial communities with a short generation time, a sessile nature and responsiveness to environmental conditions (Romaní 2010), making them ideally suited as indicators of disturbance in river systems, such as increasing temperature. Biofilms also develop rapidly on man-made surfaces, such as hydropower canals (Perkins et al. 2010) and ships' hulls (Molino et al. 2009a,b), where they constitute a biofouling problem.

The stimulating effect of temperature on growth and metabolism is well documented (Brown et al. 2004), and thus, an increase in bacterial biofilms as well as algal and protozoan biomass and activity might be expected under warming conditions. Biofilm bacterial growth rates might increase with increasing flowing water temperatures (Ratkowsky et al. 1982; Sander and Kalf 1993), but bacterial growth efficiency might decline (Sand-Jensen et al. 2007). As temperature increases all metabolic rates, it would be expected that an increase in temperature would also promote the activities of the enzymes responsible for the degradation of available organic matter. Temperature might further determine changes in the composition of bacterial species (Lindström et al. 2005; Lear et al. 2008). Ciliate growth rate and colonization would also be accelerated with increasing river water temperatures, but this would be modulated by resource availability (Weisse et al. 2002; Norf et al. 2007). In the case of algae,

*Corresponding author. Email: vdiaz@crub.uncoma.edu.ar

ISSN 0892-7014 print/ISSN 1029-2454 online

DOI: 10.1080/08927014.2010.538841
http://www.informaworld.com

temperature has been reported to increase the rates of photosynthesis, respiration and growth in phytoplankton (Findlay et al. 2001; Staehr and Sand-Jensen 2006). In biofilms, however, data on these processes in algae are few and inconsistent. On the one hand, optimum temperatures for photosynthesis vary among algal species (DeNicola 1996), so that increased temperatures could lead to a taxonomic shift instead of increased algal abundance or photosynthetic rate. In lake benthos, net photosynthesis and chlorophyll *a* (chl *a*) content may increase as a consequence of warming without an increment in total biovolume (Baulsch et al. 2005; Ventura et al. 2008). Although temperature has a positive effect on photosynthetic enzymatic activity (Davison 1991; Necchi 2006), nutrient concentration may be a limiting factor for algal growth (Christoffersen et al. 2006; Staehr and Sand-Jensen 2006), thus modulating the algal response to temperature.

The associated microbial groups (algae, bacteria and protozoa) are tightly assembled in a three-dimensional biofilm structure. The interactions between these groups might modulate the biofilm response to warming, thereby determining the outcome of the whole biofilm community (Vasseur and McCan 2005; Hansen et al. 2007). When species interact, a temperature increase can generate community changes that were not predictable from the response of a single species (Jiang and Morin 2004). In biofilms, algae and bacteria compete for nutrients (Rier and Stevenson 2002), but at the same time, bacteria make use of algal exudates, so they are positively correlated (Romaní and Sabater 1999; Carr et al. 2005). The metabolism of biofilms involves both autotrophic (photosynthesis) and heterotrophic reactions. As a consequence of a high photosynthetic rate, algal exudates may accumulate within the matrix and promote the secretion of extracellular enzymes by bacteria (Ylla et al. 2009). Increases in biofilm thickness by the growth of algae and cyanobacteria and secretion of extracellular polymeric substances (EPS) might also favor the growth of protozoa (Joubert et al. 2006). On the other hand, predation may also modify the results of the effects of temperature on the community, as protozoa play an important role in regulating the bacterial population (Norf et al. 2007; Wey et al. 2008). Temperature not only accelerates the speed of ciliate colonization (Norf et al. 2007), but also increases bacterial clearance rates (Kathol et al. 2009). However, predation by protozoa can promote mechanisms of adaptation in biofilms (Matz and Kjelleberg 2005), such as increasing cell viability (Joubert et al. 2006), which in turn could lead to changes in species composition.

The aim of this study was to evaluate the effects of a 3°C increase in temperature on biofilm structure and function in the context of a warming global change. The study considered the prediction of increases of 2–4°C in mean river water temperature (IPCC 2007). The effects of temperature on biofilm structure and function were evaluated in relation to nutrient concentration to determine the interactive effects of temperature with nutrient availability. The biomass of algae, bacteria and ciliate in biofilms as well as heterotrophic and autotrophic activities were analyzed during the colonization process. In rivers and streams, biofilm attachment, detachment and recolonization processes occur periodically, mainly due to discharge, grazing and release of dead cells when the maximum carrying capacity is reached (Stoodley et al. 2001). Furthermore, the structure of a biofilm changes with respect to its metabolism, thickness, density and composition according to how the biofilm develops (Jenkinson and Lappin-Scott 2001). Thus, an increase in the temperature of river water might affect the various steps of biofilm development differentially, thereby determining changes in the speed of accrual for the different members of the biofilm community (Romaní 2010). It is hypothesised that an increase in temperature would have more pronounced effects during the early stages of biofilm development when cells within a thinner biofilm have greater access to light and nutrients. It is predicted that if growth is limited by nutrients, temperature will exert a greater effect on biofilms at higher nutrient levels.

Methods

Experimental procedure

Biofilm colonization was analyzed in a 60-day laboratory experiment at four different conditions, viz : high temperature and high nutrients (HTHN); high temperature and low nutrients (HTLN); low temperature and high nutrients (LTHN); low temperature and low nutrients (LTLN).

Sand-blasted glass tiles (1 cm^2) were used as substrata for epilithic biofilm growth. Tiles were placed at the bottom of sterile glass jars (19 cm in diameter, 9 cm high). Each jar or mesocosm was considered a replicate, and for each treatment, three jars were established (12 mesocosms in total). Mesocosms were maintained in a constant day-night light cycle (12 h/12 h) using two incubators (SCHLAB Model PGA-500, 'Sistemas del Clima para el Laboratorio' S.L., Barcelona, Spain). The incubator for the low-temperature treatments (LTHN and LTLN) was set at 7 and 11°C during dark and light, respectively, while the incubator for high-temperature treatments (HTHN

and HTLN) was set at 11 and 15°C during dark and light, respectively. Water temperature fluctuations inside the mesocosms during the experiment were assessed with a temperature data logger (ACR SmartButton Logger, MicroDAQ, Contoocook, USA). The irradiance reaching the glass substrata was 150 μmol photons m^{-2} s^{-1}.

The mesocosms were filled with 1.5 l of artificial river water that was recirculated by means of a submersible pump (Pico 300, 230 V, 50 Hz, 4.5 W, Hydor srl, Italy). Artificial river water was obtained by dissolving pure salts (12 mg l^{-1} Na_2SO_4, 20 mg l^{-1} Na_2SiO_3, 30 mg l^{-1} $CaCl_2$, 1 mg l^{-1} KCl, 2 mg l^{-1} $MgSO_4$ and 20 mg l^{-1} $NaHCO_3$) in MilliQ water to reproduce the chemical composition of the Fuirosos stream where the biofilm inoculum was collected. The Fuirosos stream is an oligotrophic third-order forested stream at the north-east of the Iberian Peninsula with a mean water temperature of 16.5°C (Sabater et al. 2008). The simulated river water was sterilized by autoclaving. To promote colonization of the glass substrata, a biofilm previously scraped under sterile conditions from five rocks collected from the Fuirosos stream (15 ml, containing 45 μg of chlorophyll) was added to each mesocosm at the beginning of the experiment.

Enrichment was achieved by adding inorganic nitrogen and phosphorus at two different concentrations to the corresponding mesocosms. For the low nutrient treatments, the concentrations were 0.750 mg l^{-1} N-NH_4NO_3 and 0.054 mg l^{-1} P-PO_4, and for the high nutrient treatments, they were 7.5 mg l^{-1} N-NH_4NO_3 and 0.54 mg l^{-1} P-PO_4. To prevent phosphorus and nitrogen depletion and to maintain the imposed nutrient conditions, the water from each mesocosm was replaced by fresh sterile simulated river water 10 days after the beginning of the experiment and then every 3–4 days.

The chemical condition of the mesocosms was monitored during the experiment. Water samples from each mesocosm were filtered through a 0.2-μm pore diameter nylon filter (Whatman) to analyze inorganic nutrients. Phosphate was determined spectrophotometrically by the ascorbate-reduced molybdenum blue method (APHA 1989). Nitrate was analyzed with ionic chromatography (761 Compact IC Metrohm, Herisau, Switzerland). Ammonium was analyzed spectrophotometrically following Grasshoff et al. (1983). The oxygen concentration (Hach DO meter, Loveland, USA), pH (pH meter, Crison, Barcelona, Spain) and conductivity (conductivity meter, Hach, Loveland, USA) in the mesocosms were also analyzed.

The effects of temperature and nutrients on biofilm structure and function were monitored throughout the biofilm formation process. Glass tiles were sampled at random from each mesocosm on days 1, 2, 3, 4, 7, 14, 21, 30, 37, 44 and 58 for chlorophyll, bacterial density and extracellular enzyme activities (β-glucosidase, leucine-aminopeptidase, phosphatase). Ciliate density and diversity were estimated on days 4, 7, 14, 30, 44 and 58. Bacterial and algal diversity were analyzed in samples from days 30 and 58.

Biofilm structure was analyzed by scanning electronic microscopy (SEM, days 15 and 35) and confocal laser scanning microscopy (CLSM, day 38). At the end of the experiment, biofilm primary production and respiration were measured from the oxygen balance.

Algae, bacteria and ciliate colonization

Algal biomass and community composition

The chl *a* concentration on the glass tiles was measured after extraction in 90% acetone for 12 h in the dark at 4°C. To ensure complete extraction of chlorophyll, samples were further sonicated for 2 min in a Selecta sonication bath (J.P. Selecta S.A., Abrera, Spain) operating at 40 W and 40 kHz and protected from light. Extracts were filtered with fiberglass filters (GF/C Whatman), and the chl a concentration was then determined spectrophotometrically (Shimadzu UV-1800, Shimadzu Corporation, Kyoto, Japan), following Jeffrey and Humphrey (1975).

One glass tile from each mesocosm was preserved in formalin (4%) in order to determine the algal composition. Glass substrata were sonicated for 2 min using the same ultrasonication bath as above (Selecta, 40 W, 14 Khz) to achieve complete detachment of the microbial community and then observed under a light microscope (Nikon E600, Nikon Corporation, Tokyo, Japan) at 400×. Algal community composition was determined qualitatively after colonization for 30 days.

Bacterial biomass and community composition

Live and dead bacteria were counted using the Live/Dead Baclight bacterial viability kit (Invitrogen® Molecular probes, Invitrogen S.A., Barcelona, Spain) (Freese et al. 2006). Bacterial density was estimated after adding 2 ml of autoclaved MilliQ water to each tile and detaching the biofilm with a sterile cell scraper. After appropriate dilution of the biofilm suspension with sterile water (1:10 dilution was necessary from day 7 of colonization), a 1:1 mixture of SYTO® 9 and propidium iodide was added to the sample and incubated for 15 min in the dark. Samples were then filtered (0.2-μm pore diameter black polycarbonate filters, Nucleopore, Whatman), and at least 15 randomly chosen fields were counted for each slide (Nikon E600 epifluorescence microscope). Bacterial

total density was calculated as the sum of live and dead bacteria and expressed as cell per cm^2 of biofilm. The fraction of live bacteria was calculated as the abundance of live cells divided by the total counts obtained with the live/dead method.

Bacterial community structure and composition was determined on day 30 and 58 samples. Tiles (one tile from each mesocosm) were scraped in 1 ml of MilliQ water, and samples were frozen until analysed. Bacteria were determined by denaturing gradient gel electrophoresis (DGGE). The universal primers 27F (5′-AGA GTT TGA TC(AC) TGG CTC AG-3′) with a degenerate base pair at one position with a GC-clamp (5′-CGC CCG CCG CGC CCC GCG CCC GTC CCG CCG CCC CCG CCC G-5′) spanning *Escherichia coli* positions 8–27 and 517R (5′-ATT ACC GCG GCT GCT GG-3′) spanning *E. coli* positions 518–534 were used for amplification of a 566-bp long fragment of the 16S rDNA of Eubacteria. PCR was performed as follows: an activation step for the polymerase for 15 min at 95°C, 35 cycles with initial denaturation for 30 s at 94°C, annealing for 30 s at 54°C and elongation for 1.5 min at 72°C, followed by a final elongation step for 7 min at 72°C. The PCR mix contained 2 μl of the template, 1.25 U of the HotStar DNA Taq polymerase (PeqLab, Erlangen, Germany), 1 μl of dNTPs (0.2 mM final concentration per vial and dNTP), 1.5 μl of each primer (20 pM final concentration per vial), and 5 μl of reaction buffer (10X), with the total volume being 50 μl.

DGGE analysis of the PCR products (15–25 μl) was performed by means of the D-Code-System (BioRad Laboratories GmbH, Munich, Germany) using polyacrylamide gels containing a 40–70% urea gradient. DGGE gels were run in 1 × TAE buffer (40 mmol l^{-1} Tris, 20 mmol l^{-1} acetate, 1 mmol l^{-1} EDTA) at 70 V and 60°C for 16 h. The gels were stained with SYBR® Gold (Invitrogen, Karlsruhe, Germany). The stained gels were immediately analyzed using the Lumi-Imager Working Station (Roche Diagnostics, Mannheim, Germany). DGGE fingerprints were scored manually by the presence or absence of DNA bands. Intensively stained bands were excised from the DGGE gel, and the gel slices were equilibrated in 15 μl of sterile water overnight at room temperature. The DNA extract was re-amplified by PCR and subjected to DGGE again to verify the purity of the PCR re-amplification product. PCR products were purified using a ExoSap kit (usb, Staufen, Germany). The sequencing reaction was carried out using the BigDye® Terminator v1.1 Cycle Sequencing Kit (Applied Biosystems), and sequence detection was accomplished using the ABI Prism 310 genetic analyzer (Applied Biosystems) according to the manufacturer's protocol. DNA identification was achieved by comparing the nucleic acid sequences with GenBank sequences using the BLAST program (http://www.ncbi.nlm.nih.gov).

Ciliate density

For ciliate determination and counting, observations were carried out on live specimens. Tiles from each treatment were scraped (sterile cell scraper) in 1 ml of autoclaved water. The whole sample was obtained using a Pasteur pipette, and the material was allowed to sediment at the edge of the pipette for several minutes. Two separate drops from the edge of the pipette (containing all of the settled material from the 1 ml sample) were prepared for observation and counting under an optical microscope (400X Nikon eclipse 80i). Identification of ciliates was performed following Foissner and Berger (1996), and the relative contribution of the most common subclass (Peritrichia, Hymenostomatia, Hypotrichia) was calculated.

Biofilm structure

CLSM observations

CLSM was performed to establish possible differences between treatments in the spatial organization, architecture and depth profiles of biofilms. On day 38, one glass tile per treatment was collected and transferred into individual flasks with enough water for the sample to be analyzed *in vivo* by CLSM (Leica TCS-SP5 (Leica Microsystems Heidelberg GmbH, Mannheim, Germany). Autofluorescence of photosynthetic pigments was detected using the 561- (phycobiliproteins) and 633- (chlorophylls) nm lines of an Ar/HeNe laser (excitation) and observed in the red and far red channels at 590 to 800 nm (emission). The location of the EPS in the biofilms was detected by staining with the carbohydrate recognition compound lectin concanavalin A (ConA)-Alexa Fluor 488 (Molecular Probes, Inc., Eugene, OR), excited with the 488-nm line of an Ar laser, and observed in the green channel at 490 to 530 nm. DNA was stained with Hoechst (Hoechst 33342, Molecular Probes, Invitrogen, H-3570), excited by ultraviolet light at 405 nm, and observed in the blue/cyan fluorescence light around an emission maximum at 414–458 nm. For image analysis, three dimensional images were recorded for each treatment at each 5-μm interval. Image analyses were performed with the IMARIS program (v. 6.1.0 software, Bitplane, Zürich, Switzerland). Biofilm thickness was determined as the distance between the top of the biofilm and the glass.

SEM observations

Samples for SEM (one glass tile from each treatment collected after incubation for 15 and 35 days) were fixed immediately after sampling with 2.5%

glutaraldehyde in 0.1 M cacodylate buffer, pH 7.2–7.4. Afterwards, a series of ethanol baths (65 to 100%) were used to dehydrate the samples, which were further dried by critical point drying with CO_2. Samples were coated with gold using a sputtering diode and observed under a Zeiss DSM 960 SEM.

Biofilm function

Extracellular enzyme activities

The extracellular enzyme activities of β-D-1,4-glucosidase, phosphatase and leucine-aminopeptidase were measured spectrofluorometrically using 4-methylumbelliferyl-β-D-glucopyranoside, methylumbelliferyl-phosphate and 7-aminomethylcoumarin-leucine (Sigma-Aldrich) as substrate analogues. Glass substrata (1 tile per mesocosm and at each sampling date) were collected for the incubations. Enzyme activity incubations were performed with a 0.3 mM substrate concentration (saturation conditions; Romaní et al. 2004) in the dark under continuous shaking for 1 h at 11 and 15°C for each temperature treatment immediately after sampling. Blanks and standards of MUF (methylumbelliferone) and AMC (aminomethylcoumarin) were also included. At the end of the incubation, glycine buffer (pH 10.4) was added (1:1 v/v) and fluorescence was measured at 365/455 nm and 364/445 nm excitation/emission for MUF and AMC, respectively (Kontron SFM 25). Blanks consisted of water from the same mesocosms. The fluorescence intensity of the blanks was subtracted from all the samples to correct for hydrolysis of the substrate or fluorescent substances in the water solution. Values were expressed as nmol MUF or AMC $cm^{-2}\ h^{-1}$.

Primary production and respiration

Primary production and photosynthetic activity were measured on day 48. To estimate primary production by oxygen balance, two colonized glass tiles from each mesocosm were randomly selected and placed in 50-ml flasks. First, total community respiration (R) was calculated by incubating the tiles in darkness (two hours before the lights were turned on) for 1.5 h. Dissolved oxygen concentration in the water was measured with an oxygen probe (WTW Oxi 340-A) at the beginning and at the end of the incubation. Net primary production (NPP) was calculated in the same manner, but 4 h after the lights were turned on. The gross primary production (GPP) was calculated as the difference between NPP and R and expressed as mg $O_2\ cm^{-2}\ h^{-1}$.

Statistical analyses

The time sequence for development of bacterial density and accumulation of chl *a* was analyzed by non-linear regression and fit to a sigmoid curve (three parameters). The parameters K (carrying capacity), r (growth rate) and X_0 (time when maximal growth rate was achieved) were estimated using SigmaPlot graph software (Systat Software, Inc., San Jose, CA, USA). These parameters were calculated for each curve ($n = 3$ per treatment) and compared among treatments with two-way ANOVA to reveal statistical differences.

The effects of temperature at the different nutrient levels on chlorophyll *a* concentration, bacterial density, ciliate abundance, and extracellular enzyme activities throughout biofilm formation were analyzed by repeated measures analysis of variance (two-way RM-ANOVA, temperature and nutrient factors) using SPSS. Statistical differences between treatments for primary production and respiration were analyzed by a two-way ANOVA. All variables included in the analyses were log (x) transformed, except for chl *a*, which was log ($x + 1$) transformed.

To analyze bacterial diversity, similarity patterns were calculated with the Sorensen coefficient: $Cs = 2j(a + b)^{-1}$, where j is the number of common DGGE bands between samples A and B, and a and b are the number of bands in samples A and B, respectively (Murray et al. 1996). This index ranges from 0 (no common bands) to 1 (100% similarity of band patterns). Dendrograms were built based on the complete linkage method with the Primer 6 & Permanova + program (PRIMER-E, Ltd). The number of different DGGE bands obtained for the different treatments were compared by a t-test.

Results

Physical and chemical conditions in the mesocosms

The water temperature inside the mesocosms was slightly higher than that programmed into the incubators as detected by the temperature data loggers submerged in the mesocosms. The high temperature treatments were at 16.0 ± 0.57°C (day) and 14.71 ± 0.42°C (night), and the low temperature treatments were at 13.19 ± 1.48°C (day) and 11.10 ± 0.93°C (night), with $n = 1221$ for each treatment. Thus, the difference between treatments was approximately 3°C (2.81 during the day, 3.61 during the night).

During the experiments, conductivity, pH and oxygen within the mesocosms remained steady at 120–140 μS cm^{-1}, 7–7.7 and 9.4–10.7 mg l^{-1}, respectively. Nutrient content, especially phosphate concentration, decreased in each 3–4 day period (from 0.054 and 0.540 mg l^{-1} to < 10 μg l^{-1}), but nutrient depletion was prevented by periodic water replacement at the same time interval. The nitrogen content in the mesocosms was slightly lower than the imposed

conditions (from 0.750 and 7.5 mg l^{-1} N-NH_4NO_3 to 0.542 and 4.154 mg l^{-1} on average after each 3–4 day period, for high and low nutrient conditions respectively). Water replacement was necessary to maintain the imposed nutrient conditions.

Colonization by algae, bacteria and ciliates

Accumulation of algal biomass on tiles was greater at the higher nutrient condition, and colonization was earlier and faster at the higher temperature (Figure 1, Table 1, nutrient and temperature × nutrient interaction effects). Development of chl *a* over time fitted to a sigmoid function at the four treatments is shown in Figure 1 and Table 2. The estimated parameters of the curve indicate a significantly earlier maximum algal accrual (lower values of X_0) and higher maximum growth rate (r) for the biofilms grown at higher temperatures, independent of nutrient level (two-way ANOVA, temperature effect, $p = 0.014$ and $p = 0.021$, for X_0 and r, respectively; no significant effect for nutrients or for temperature x nutrient interaction).

The algal composition on day 30 revealed a high density of the filamentous cyanobacterium *Phormidium* sp. in the high temperature treatment (Figure 2); other cyanobacteria observed were *Oscillatoria* sp. and an unidentified member of the Chroococcales. Diatoms (almost 100% *Achnanthidium minutisimum*) were present in all treatments, but they were abundant only in treatment LTLN (almost 90%). Most of the chlorophytes belonged to the class Chlorococcales and were abundant in all treatments. The filamentous alga *Stigeoclonium* sp. was frequent only when nutrient levels were low, especially at high temperatures (Figure 2). *Bothriococcus* sp. (Xanthophyceae) was also abundant in all treatments except in LTLN.

The bacterial total density increased earlier than chl *a*, and no significant differences between the two temperature treatments or between the two nutrient concentrations were found (Table 1). Bacterial density values fitted to a sigmoid function for the four treatments are shown in Figure 1 and Table 2. In the HTHN treatment, an earlier maximum growth (lowest X_0) and highest maximum growth (r) were observed (Table 2), though the differences were not statistically significant (two-way ANOVA, $p > 0.1$). In all treatments, the percentage of live bacteria showed no significant differences (Table 1). Live bacteria accounted for 34.2% ± 3.2 of the bacteria on average for the whole experiment and maximum values were obtained at day 7 of colonization (average 55.3%). No significant differences between treatments were measured for live bacteria (RM-ANOVA, $p > 0.1$).

Bacterial diversity changed during biofilm colonization such that at day 30, the most important factor determining community assemblage was temperature, and two groups were clearly defined (with <40% similarity, Figure 3). The total number of DGGE bands at high temperatures was 19.6 ± 1.5 when low nutrients were available and 22.3 ± 2.3 with high nutrient concentrations. At low temperature, the total DGGE bands were 20.6 ± 1.3 and 17.3 ± 0.6 with high nutrients and low nutrients, respectively. DNA

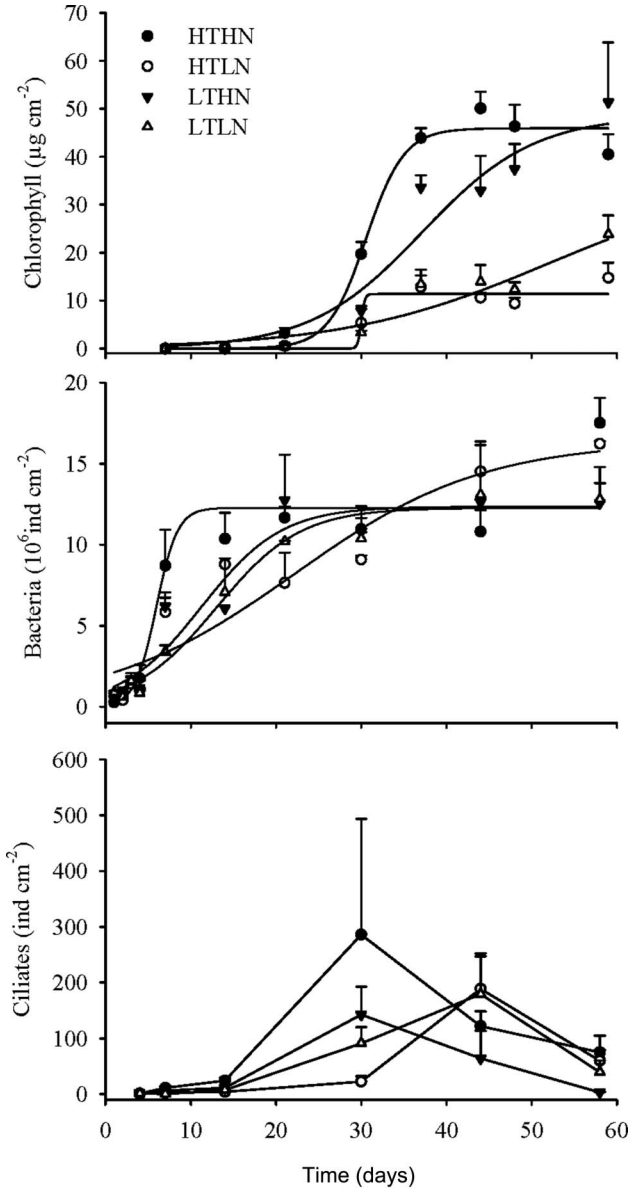

Figure 1. Colonization by algae (chlorophyll concentration), bacteria and ciliates (individuals per cm^2) for the different treatments (HTHN = high temperature high nutrients, HTLN = high temperature low nutrients, LTHN = low temperature high nutrients, LTLN = low temperature low nutrients). Data are means ±1 SE ($n = 3$). The sigmoid model is fitted for bacteria and chl *a* and parameter estimates of the non-linear regression indicated in Table 2.

Table 1. Results of repeated-measures ANOVA on chlorophyll, bacterial, ciliate and extracellular enzyme activities during biofilm formation.

Source of variation	Chlorophyll	Bacteria	Ciliates	β-Glucosidase	Peptidase	Phosphatase
Day						
Temperature (T)	0.448	0.990	0.956	0.929	*0.067*	0.259
Nutrients (N)	**<0.001**	0.433	0.997	**0.020**	**<0.001**	0.904
Day × T	0.274	0.861	0.999	0.365	0.894	0.830
Day × N	**<0.001**	0.988	0.610	0.316	0.113	**<0.001**
T × N	*0.057*	0.999	0.842	0.975	*0.014*	0.416
Day × T × N	0.855	0.969	0.990	0.824	0.913	0.981

Temperature (T) and nutrient (N) effects, as well as interactions with colonizing day (Day) were evaluated. Probability within groups (Day and interactions Day × T, Day × N, and Day × T × N) are corrected for sphericity by the Greenhouse–Geisser correction. All probabilities are adjusted by the Dunn–Sidak correction. Values <0.05 are indicated in bold, and those <0.1 are indicated in italics.

Table 2. Parameter estimates for non-linear regression of chl *a* concentration and bacterial abundance throughout biofilm formation (sigmoid model, 3 parameters, $N = K/(1 + \text{e exp } (-((x-X_0)/b))$.

	HTHN	HTLN	LTHN	LTLN
Chl *a*				
R^2	0.98	0.93	0.94	0.91
p	<0.0001	0.0012	0.0007	0.0023
X_0 (day)	30.65 ± 0.35	29.93 ± 1.75	39.61 ± 4.42	47.79 ± 7.14
r (day^{-1})	1.33 ± 0.90	1.42 ± 0.90	0.26 ± 0.14	0.19 ± 0.10
Bacterial abundance				
R^2	0.89	0.87	0.84	0.98
p	0.0005	0.0008	0.0016	<0.0001
X_0 (day)	6.15 ± 1.00	18.30 ± 4.40	14.28 ± 5.57	12.51 ± 2.68
r (day^{-1})	1.00 ± 0.20	0.14 ± 0.04	0.31 ± 0.13	0.28 ± 0.07

The parameters X_0 (day when maximal growth rate is achieved) and r (= $1/b$, maximum growth rate) are indicated ($n = 3$ for each treatment). The coefficients of determination (R^2) and significance of F-Fischer (probability, p) are also shown.

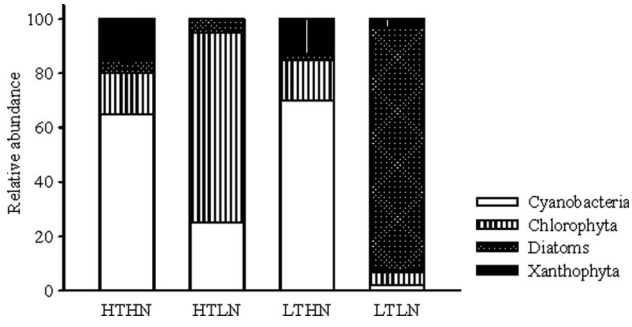

Figure 2. Relative abundance of the algal groups Xanthophyta, Diatoms, Chlorophyta and Cyanobacteria in the four treatments (HTHN = high temperature high nutrients, HTLN = high temperature low nutrients, LTHN = low temperature high nutrients, LTLN = low temperature low nutrients).

bands (22 in total, 8 bands in day 30 and 14 bands in day 58 samples) were excised and sequenced for taxonomic identification. *Hydrogenophaga, Pseudomonas putida, Acidovax* spp., *Roseomonas frigidaquae* and *Rhodoferax* spp. could be identified in the samples, especially under high temperature conditions. In contrast, on day 58, the bacterial assemblages were mostly determined by nutrient treatments (Figure 3). In this case, the total number of DGGE bands under high nutrients was 12.3 ± 0.3 at low temperature and 13.6 ± 1.9 at high temperature, and under low nutrients the number of DGGE bands was 14.6 ± 1.6 and 14.3 ± 2.3 at low and high temperature, respectively. No significant differences in the number of DGGE bands between treatments were detected for any of the two sampling dates (t-test, $p > 0.1$). Compared with 30-day-old biofilms, the total number of DNA bands representing the total numbers of different Eubacteria in the biofilms on day 58 was significantly lower (*t*-test, $p < 0.001$). The specific DNA bands were also sequenced. One sequence alignment showed approximately 99% similarity with *Acidovorax temperans*, but most of the sequence data matched with uncultured Proteobacteria.

Ciliate abundance showed no significant differences between treatments (Table 1), although an initial increase was clearly observed on day 30 in the high nutrient treatments and especially at higher temperatures (HTHN treatment, Figure 1). On the first

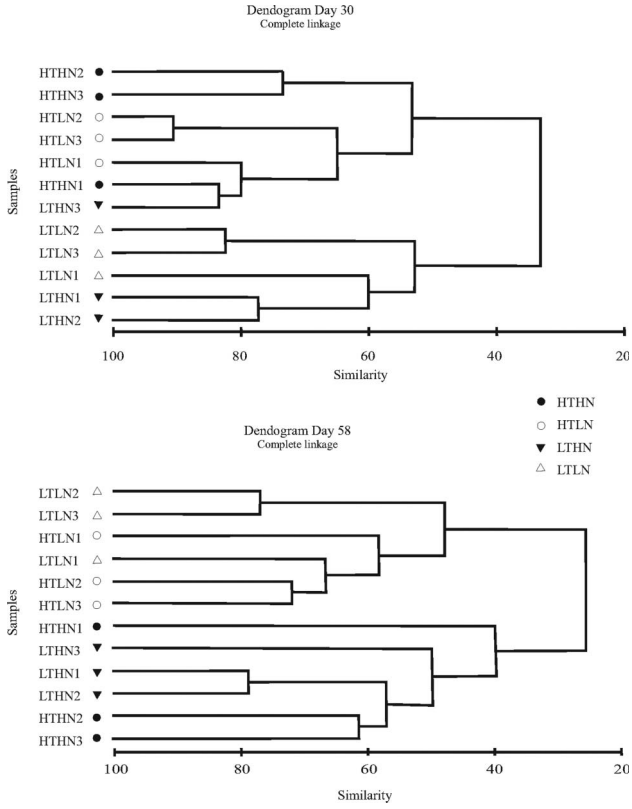

Figure 3. Dendograms of bacterial diversity (days 30 and 58) based on the complete linkage method calculated with the Sorensen similarity index for the bands of DGGE. HTHN = high temperature high nutrients, HTLN = high temperature low nutrients, LTHN = low temperature high nutrients, LTLN = low temperature low nutrients. Numbers correspond to replicates.

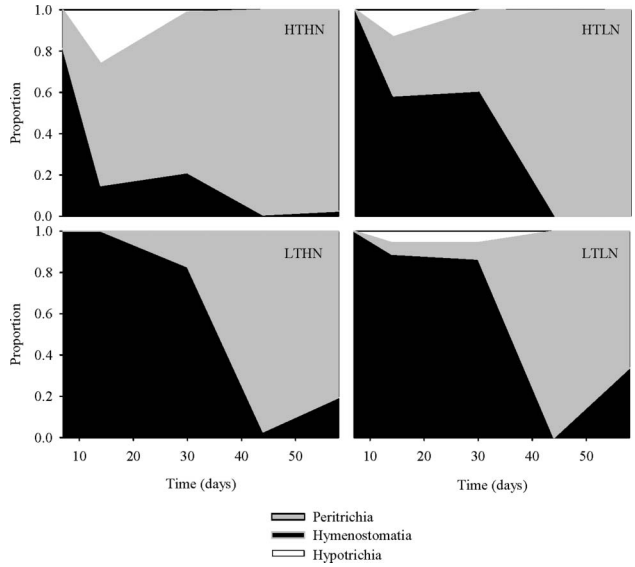

Figure 4. Relative abundance of the ciliate groups Peritrichia, Hymenostomatia and Hypotrichia during colonization in the different treatments (HTHN = high temperature high nutrients, HTLN = high temperature low nutrients, LTHN = low temperature high nutrients, LTLN = low temperature low nutrients). Data are means $\pm$ 1 SE ($n = 3$).

sampling dates, hymenostomata dominated the assemblages in all treatments; subsequently, peritrichia became dominant, first in the HTHN treatments (day 14), then in HTLN and finally in the LTHN and LTLN treatments (Figure 4). The larger abundance of peritrichia (mainly *Vorticella* sp.) in the HTHN treatment was also confirmed by SEM (images from day 15 and 35, not shown) and CLSM observations (images from day 38, Figure 5).

Biofilm structure as qualitatively analyzed by SEM observations on day 15 of colonization confirmed the earlier colonization of the glass tiles under HTHN conditions, while biofilms grown at low nutrient concentrations revealed a poorly colonized matrix of mucilaginous matter, and empty spaces could be observed. The three dimensional analysis of the biofilms imaged by CLSM on day 38 revealed a thicker development in the higher temperature treatments (both at higher and lower nutrient levels, Figure 5). In addition to differences in biofilm thickness, the contribution of algae, cyanobacteria, heterotrophic organisms (non-photosynthetic bacteria and protozoa) and EPS were observed (Figure 5). At high nutrient concentrations, temperature had a significant effect on the density of peritrichia, which can be distinguished in the CLMS images by a C-shaped nucleus.

Biofilm function

Extracellular enzyme activity increased as the biofilms developed (Figure 6). The activity of β-glucosidase was not affected by temperature, but it was significantly higher in high nutrient treatments (RM-ANOVA, Table 1). The positive effect of temperature on leucine aminopeptidase was significant at high nutrient conditions (RM-ANOVA, temperature x nutrient interaction effect, Table 1). Thus, the highest values were reached in the HTHN treatment. Additionally, the two individual factors, temperature and nutrients, also enhanced peptidase activity (Table 1). Phosphatase activity showed a different time pattern depending on nutrient treatment such that at high nutrient level the activity was saturated after 1week, while at low nutrient, phosphatase activity was still increasing at the end of the experiment (Figure 6, Table 2).

Biofilm gross primary production and respiration on day 48 were slightly higher in the HTHN treatment, but differences between treatments were not significant (Figure 7, ANOVA, $p > 0.1$). However, gross primary

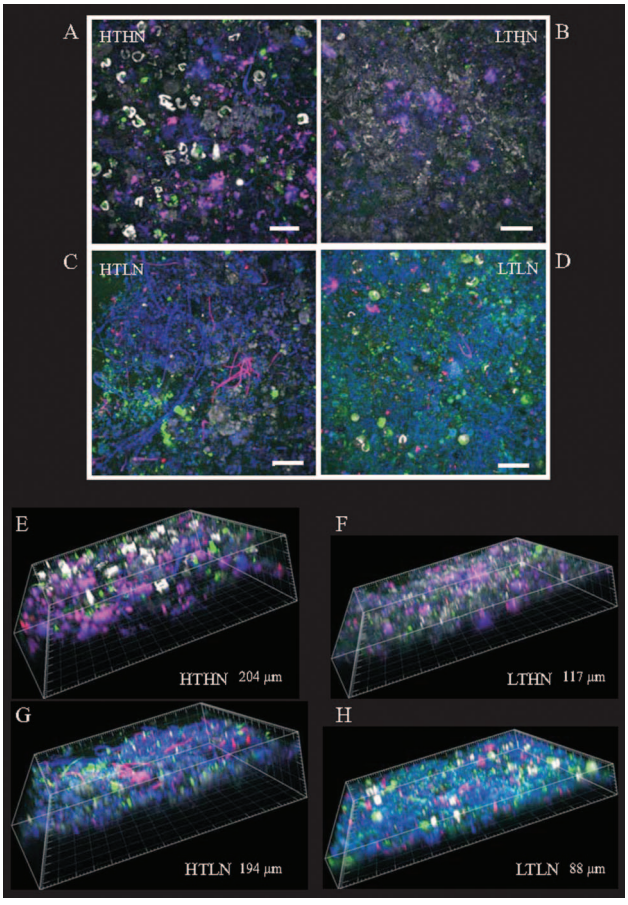

Figure 5. CLSM images at day 38 of colonization (HTHN = high temperature high nutrients, HTLN = high temperature low nutrients, LTHN = low temperature high nutrients, LTLN = low temperature low nutrients). Autofluorescence of photosynthetic pigments was registered in blue (chlorophylls) and pink (phycobiliproteins from cyanobacteria). The location of the EPS in the biofilms is shown in green and DNA in grey. For image analysis, three dimensional images (E–H) were recorded for each treatment at 5 μm intervals. Scale = 100 μm.

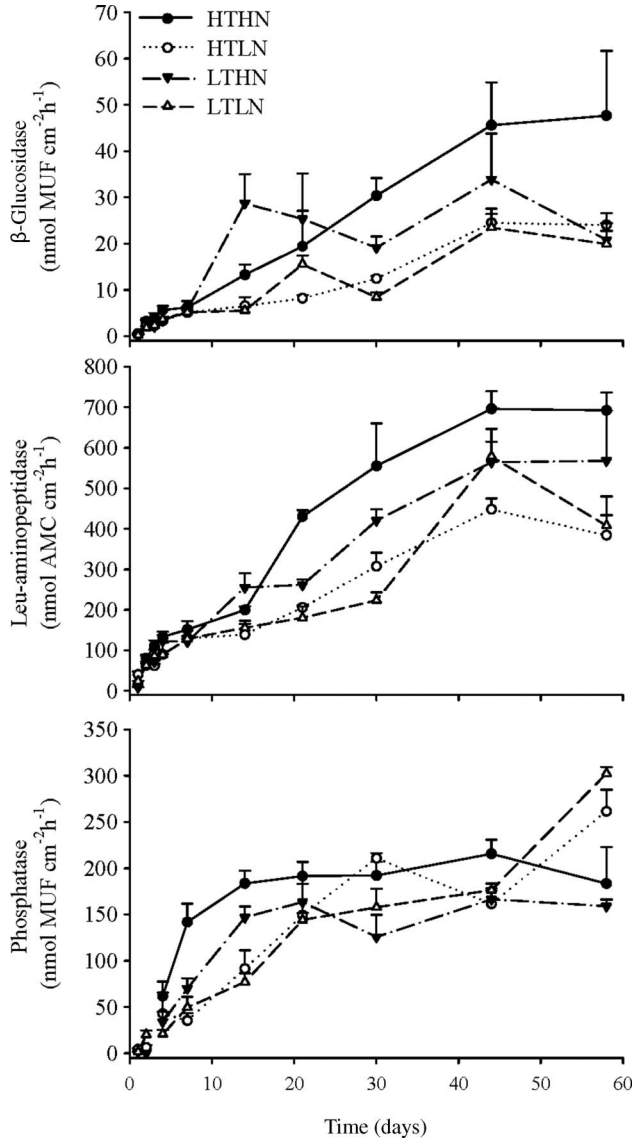

Figure 6. Extracellular enzymatic activities (β-D–1,4-glucosidase, phosphatase and leucine-aminopeptidase) during biofilm colonization in treatments HTHN = high temperature high nutrients, HTLN = high temperature low nutrients, LTHN = low temperature high nutrients and LTLN = low temperature low nutrients. Data are means $\pm$ 1 SE (n = 3).

production per unit of chl *a* was significantly higher at low nutrient levels (ANOVA, $p = 0.003$), though it was not affected by temperature.

Discussion

Biofilm formation was faster and microbial colonization of the substratum occurred earlier when the temperature of flowing water was increased by 3°C. Significant effects on the colonizing dynamics of the three groups (algae, bacteria and ciliates) were seen, but their response to increased temperature was modulated by interactions between them. However, temperature did not affect the final biomass of the biofilm. The population size at which growth stops is known as the carrying capacity, or K, which is the number of individuals of a particular population that the environment can support. In the experiment described, the biofilm carrying capacity under the two temperature conditions was the same.

Bacterial and algal colonization patterns showed typical colonization dynamics, with an initial low grow phase, an exponential growth phase and a stabilization phase (Romaní 2010). The biofilm was first dominated by bacteria (until approximately day 20), and later, algal growth accelerated as shown by Battin et al. (2003). This pattern was clearly affected by the increase

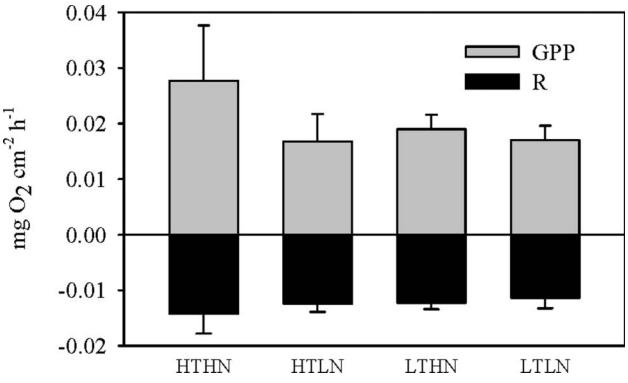

Figure 7. Gross primary production (GPP) and respiration (R) in treatments HTHN = high temperature high nutrients, HTLN = high temperature low nutrients, LTHN = low temperature high nutrients and LTLN = low temperature low nutrients on day 48. Data are means ± 1 SE ($n = 3$).

in temperature, as shown by the earlier colonization by all three microbial groups at the higher temperatures, particularly in the higher nutrient treatment.

Algal biomass accumulation in biofilms was determined to a great extent by nutrient availability. The algal carrying capacity (chl *a*) clearly increased under high nutrient conditions (Romaní 2010). Nevertheless, algal colonization was significantly faster at the higher temperature, independent of nutrient availability. Increases in algal biomass with temperature increases have been previously described (DeNicola 1996). The rapid algal colonization under higher temperatures led to the biofilm reaching its carrying capacity earlier, which was also indicated by the dislodgment commonly observed at the last sampling day in the higher temperature treatments. When a biofilm becomes thicker, detritic material and dead cells accumulated in the lower layers cause loss of stability, and part of the biomass sloughs off (Xavier et al. 2005). However, under the lower temperature, chl *a* was still increasing at the end of the experiment, reaching a similar level to that in the higher temperature condition. Therefore, increased temperature accelerated algal colonization, but did not affect the carrying capacity of the biofilm. However, the effect of temperature on chl *a* levels throughout the biofilm formation process was only significant under high nutrient availability, suggesting that if nutrients are a limiting factor, increases in water temperature might not lead to an increment in algal growth rate (Raven and Geider 1988). Nutrient limitation in the low nutrient treatment was indicated by phosphatase activity, which was still increasing at the end of the experiment indicating the acquisition of inorganic phosphorus from organic compounds.

Increased temperature accelerated algal growth, but the effect on gross primary production was not significant. In contrast, Christoffersen et al. (2006) and Staehr and Sand-Jensen (2006) found that temperature enhanced primary production of phytoplankton. This discrepancy may be explained by the effects of temperature on three-dimensional biofilm structure and the composition of primary producers. Although biofilm thickness as measured by CLSM should be viewed with caution because it is highly dependent on the capacity of the laser to penetrate into the biofilm (Barranguet et al. 2004), since the images were analyzed the same day with the same microscope and laser conditions, the results showing a doubling of biofilm thickness under warming conditions are considered robust. Similar results of increased thickness were observed for biofilms affected by nuclear power plant effluents that increased the water temperature by about 5°C (Rao 2010). Since under warming conditions (independently of nutrient availability), a thicker biofilm was formed, but with similar biomass, the biofilm structure might be less dense at increased temperature. Increases in biofilm thickness could cause primary producers buried and shaded in the lower layers of the biofilm to be less productive than those that are fully exposed in the upper layers, resulting in similar primary productivities of the different biofilms at the end of the experiment. The lack of effect on primary production could also be related to changes in the primary producer composition. Falk et al. (1996) stated that it is not possible to describe a general mechanism for photosynthetic adjustment to temperature that encompasses all autotrophic species because of genetic diversity and differential strategies in growth and development. In the present study, although similar species were found, their contribution clearly differed between treatments. Filamentous forms were more abundant at higher temperatures (Cyanobacteria and *Stigeoclonium*), while the contribution of diatoms was lower, thus following the general pattern described for an algal community response to increasing temperatures (Patrick 1969).

Surprisingly, bacterial abundance over the course of the whole biofilm formation process was not significantly affected by temperature or by nutrients. Numerous studies have reported positive effects of temperature on bacterial growth (Ratkowsky et al. 1982, Sander and Kalff 1993; Lindström et al. 2005). In the present study, although a greater bacterial growth rate and earlier bacterial colonization at higher temperature and higher nutrient conditions were measured, this was not translated into accrual of higher bacterial biomass. The percentage of live bacteria fell within the range described for biofilms (20-70%, Romaní 2010) and any significant effect of the imposed treatments on bacterial cell viability was

detected. Cell lysis frequently occurs in biofilms and percentages of 50% of dead bacteria throughout biofilm colonization have been measured (Romaní et al. 2008). Bacterial cell death is important for biofilm development and autolysis can promote biofilm formation because of the release of cell contents (Tresse et al. 2003; Bayles 2007).

Additionally, because of the well-known positive interaction between algae and bacteria in biofilms, a greater bacterial density in the higher nutrient treatments would be expected. Bacteria in biofilms are favored by algae, as they use algal exudates as a carbon source (Romaní and Sabater 1999; Carr et al. 2005; Scott et al. 2008). Thus, leucine-aminopeptidase was increased with higher temperatures, especially under high nutrient conditions, indicating a greater use of released algal peptides (Ylla et al. 2009). Therefore, the same bacterial density supports a higher peptidase activity in this case, indicating greater activity per bacterial cell. In addition, the expected stimulation of enzyme activity at higher temperatures was mainly observed at high nutrient levels. The lack of a positive response by β-glucosidase and peptidase to temperature at low nutrient concentrations may be related to the lower availability of substrates for these enzymes (polysaccharides and peptides) under lower nutrient availability, where a thinner biofilm was developed.

Overall, the increase in algal biomass, bacterial growth, and β-glucosidase and leu-aminopeptidase activities would suggest a greater bacterial cell density in biofilms developed at higher nutrient conditions, especially at higher temperature. The most plausible explanation for the lack of an increase in bacterial density is greater grazing by protozoa at high nutrient and, especially, at high temperature. Protozoa might control the accrual of bacterial biomass in biofilms growing under higher nutrient conditions, but a further and significant specific effect of ciliates, especially peritrichia, is suggested at higher temperature because these organisms also increased earlier. Although direct ciliate counting showed a large variability (no statistical differences between treatments), the tendency to greater ciliate abundance at higher temperature and especially under higher nutrient availability was confirmed by both SEM and CLSM observations. Warming temperatures promote the acceleration of ciliate colonization speed (Norf et al. 2007), and bacterial enrichment leads to communities dominated by peritrichia (Norf et al. 2009). Although they are filter feeders and usually feed on bacteria from the water column (Finlay and Esteban 1998), peritrichia produce very strong feeding currents (Fenchel 1986), and as observed in CLSM images, they lived inside the biofilm matrix. Thus, it is likely that peritrichia can dislodge bacterial cells from the biofilm and so, they indirectly feed on biofilm-associated bacteria. Temperature has been shown to increase the rate of bacterial clearance by ciliates (Kathol et al. 2009), so it is suggested that ciliate grazing masks the positive effect of temperature on the rate of bacterial growth.

The lack of differences in bacterial abundance among treatments can be contrasted with changes in bacterial composition. On day 30, bacterial communities were clearly separated by the distinct temperature treatments, while at the end of the experiment, temperature was a secondary discriminating factor after the bacterial communities were separated by nutrient conditions. Changes in bacterial community composition might be a direct effect of temperature or an indirect effect of ciliate grazing. In a field study, stream temperature was found to be the most important determinant of bacterial community variability (Lear et al. 2008). On the other hand, the pressure of protozoa at HTHN conditions might also determine changes in the composition of the bacterial community. Matz and Kjelleberg (2005) suggested that protozoan predation could promote the evolution of diverse adaptive mechanisms in bacterial biofilms.

The outcome of this laboratory experiment cannot be linked to natural aquatic ecosystems without caution. In this study, allochthonous organic matter was not considered, and it has been shown that the availability of organic matter with respect to both quantity and quality affects biofilm composition and metabolism (Romaní et al. 2004, Ylla et al. 2009). Nevertheless, the results suggest that the response of aquatic biofilms to increasing water temperature will be highly modulated by interactions between the biofilm components. At higher temperatures, the faster colonizers correspond to a distinctive bacterial community that develops alongside greater colonization by peritrichia and algae, which produces a thicker (and probably less dense) biofilm. Species community composition may affect the use of organic matter within a biofilm (Olapade and Leff 2005), thus affecting processing of organics in the ecosystem. Furthermore, the development of a differential biofilm might affect the trophic web by changing biofilm palatability. However, the effects of temperature on biofilm function were more subtle, only slightly affecting extracellular enzyme activities related to the increased use of polysaccharides and peptides. It is likely that primary production and respiration during the colonization process would have been affected by temperature, but the results at the end of the biofilm formation process might be buffered by the distinctive structural characteristics of the biofilms. This 'buffer' response when considering three trophic levels demonstrates that a significant effect of warming on only one

biofilm compartment cannot be easily extrapolated to the response of the whole biofilm.

At the same time, the significant effect of warming on the dynamics of biofilm formation might determine the extent of cover of a stream bed on a long-term basis due to a fast recovery after disturbance (high flood events and/or high grazing pressure), thereby reducing the length of the lag phase needed for recolonization. Although temperature did not affect the maximum carrying capacity of the biofilm, rapid recolonization might result in a greater biofilm biomass in a stream over the long term. If global change leads to more climatic disturbance (droughts, flooding), and if biofilms can recover quickly, then the present findings suggest an increment in the available biomass for higher trophic levels in streams. Furthermore, the present results demonstrate that nutrient availability produces a greater response to warming. Therefore, warming effects would be expected to be more relevant under eutrophic conditions.

Acknowledgements

This study was funded by the project CGL2008-05618-C02-01/BOS of the Spanish Ministry of Science and Technology. A. Gaudes is acknowledged for valuable assistance with protozoan identification. J. Varela is acknowledged for her help in DGGE analysis. Thanks to M. Roldán from the Microscopic Services at the Universitat Autònoma de Barcelona for her assistance in the CLSM observations. S. Sabater is acknowledged for allowing the authors to use the ICRA facilities. V. Díaz Villanueva received a grant to participate in this project (CONICET) and is supported by FONCYT (Argentina) (Grant #PICT-2007-01747).

References

American Public Health Association (APHA). 1989. Standard methods for the examination of water, sewage, and wastewater. Washington (DC): American Public Health Association.

Barranguet C, von Beusekom SAM, Veuger B, Neu TR, Manders EMM, Sinke JJ, Admiraal W. 2004. Studying undisturbed autotrophic biofilms: still a technical challenge. Aquat Microb Ecol 34:1–9.

Battin TJ, Kaplan LA, Newbold JD, Hansen CME. 2003. Contributions of microbial biofilms to ecosystem processes in stream mesocosms. Nature 426:439–442.

Baulsch HM, Schindler DW, Turner MA, Findlay DL, Paterson MJ, Vinebrooke RD. 2005. Effects of warming on benthic communities in a boreal lake: implications of climate change. Limnol Oceanogr 50:1377–1392.

Bayles KW. 2007. The biological role of death and lysis in biofilm development. Nature Rev Microbiol 5:721–726.

Bott TL, Montgomery D, Arscott D, Dow C. 2006. Primary productivity in receiving reservoirs: links to influent streams. J N Am Benthol Soc 25:1045–1061.

Brown JH, Gilloly JF, Allen AP, Savage VM, West GB. 2004. Toward a metabolic theory of ecology. Ecology 85:1771–1789.

Carr GM, Morin A, Chambers PA. 2005. Bacteria and algae in stream periphyton along a nutrient gradient. Freshwater Biol 50:1337–1350.

Christoffersen K, Andersen N, Søndergaard M, Liboriussen L, Jeppesen E. 2006. Implications of climate-enforced temperature increases on freshwater pico and nanoplankton populations studied in artificial ponds during 16 months. Hydrobiologia 560:259–266.

Davison IR. 1991. Environmental effects on algal photosynthesis: temperature. J Phycol 27:2–8.

DeNicola DM. 1996. Periphyton responses to temperature at different ecological levels. In: Stevenson RJ, Bothwell ML, Lowe RL, editors. Algal ecology: freshwater benthic ecosystems. San Diego (CA): Academic Press. p. 150–183.

Falk S, Maxwell DP, Laudenbach DE, Huner NPA. 1996. Photosynthetic adjustment to temperature. In: Baker NR, editor. Photosynthesis and the environment. Dordrecht, The Netherlands: Kluwer Academic Publishers. p. 367–385.

Fenchel T. 1986. Protozoan filter feeding. Prog Protistol 1:65–113.

Findlay DL, Kasian SEM, Stainton MP, Beaty K, Lyng M. 2001. Climatic influences on algal populations of boreal forest lakes in the experimental lakes area. Limnol Oceanogr 46:1784–1793.

Finlay BJ, Esteban GF. 1998. Freshwater protozoa: biodiversity and ecological function. Biodivers Conserv 7:1163–1186.

Foissner W, Berger H. 1996. A user-friendly guide to the ciliates (Protozoa, Ciliophora) commonly used by hydrobiologists as bioindicators in rivers, lakes, and waste waters, with notes on their ecology. Freshwater Biol 35:375–482.

Freese HM, Karsten U, Schumannn R. 2006. Bacterial abundance, activity, and viability in the eutrophic river Warnow, Northeast Germany. Microb Ecol 51:117–127.

Grasshoff K, Ehrhardt M, Kremling K. 1983. Methods of seawater analysis. 2nd ed., rev. extend. ed. Weinheim: Verlag Chemie. 419p.

Hansen SK, Rainey PB, Haagensen JAJ, Molin S. 2007. Evolution of species interactions in a biofilm community. Nature 445:533–536.

Intergovernmental Panel on Climate Change. 2007. Climate change 2007: the physical science basis In: Solomon S, Qin D, Manning M, Chen Z, Marquis M, Averyt KB, Tignor M, Miller HL, editors. IPCC Fourth Assessment Report. Switzerland: IPCC. 18 p.

Jeffrey SW, Humphrey GF. 1975. New spectrophotometric equations for determining chlorophylls *a, b*, and *c* in higher plants, algae and natural phytoplankton. Biochem Physiol Pflanz 167: 191–194.

Jenkinson HF, Lappin-Scott H. 2001. Biofilms adhere to stay. Trends Microbiol 9:9–10.

Jiang L, Morin PJ. 2004. Temperature-dependent interactions explain unexpected responses to environmental warming in communities of competitors. J Anim Ecol 73:569–576.

Joubert L-M, Wolfaardt GM, Botha A. 2006. Microbial exopolymers link predator and prey in a model yeast biofilm system. Microb Ecol 52:187–197.

Kathol M, Norf H, Arndt H, Weitere M. 2009. Effects of temperature increase on the grazing of planktonic bacteria by biofilm-dwelling consumers. Aquat Microb Ecol 55:65–79.

Lear G, Anderson MJ, Smith JP, Boxen K, Lewis GD. 2008. Spatial and temporal heterogeneity of the bacterial communities in stream epilithic biofilms. Microb Ecol 65:463–473.

Lindström ES, Kamst-Van Agterveld MP, Zwart G. 2005. Distribution of typical freshwater bacterial groups is associated with pH, temperature, and lake water retention time. Appl Environ Microb 71:8201–8206.

Lock MA. 1993. Attached microbial communities in rivers. In: Ford TE, editor. Aquatic microbiology. Oxford, UK: Blackwells. p. 113–138.

Matz C, Kjelleberg S. 2005. Off the hook-how bacteria survive protozoan grazing. Trends Microbiol 13:302–307.

Molino PJ, Campbell E, Wetherbee R. 2009a. Development of the initial diatom microfouling layer on antifouling and fouling release surfaces in temperate and tropical Australia. Biofouling 25:685–694.

Molino PJ, Childs S, Eason Hubbard MR, Carey JM, Burgman MA, Wetherbee R. 2009b. Development of the primary bacterial microfouling layer on antifouling and fouling release coatings in temperate and tropical environments in Eastern Australia. Biofouling 25:149–162.

Murray AE, Hollibaugh JT, Orrego C. 1996. Phylogenetic compositions of bacterioplankton from two California estuaries compared by denaturing gradient gel electrophoresis of 16S rDNA fragments. Appl Environ Microbiol 62:2676–2680.

Necchi O. 2006. Photosynthetic responses to temperature in tropical lotic macroalgae. Phycol Res 52:140–148.

Norf H, Arndt H, Weitere M. 2007. Impact of local temperature increase on the early development of biofilm-associated ciliate communities. Oecologia 151:341–350.

Norf H, Arndt H, Weitere M. 2009. Responses of biofilm-dwelling ciliate communities to planktonic and benthic resource enrichment. Microb Ecol 57:687–700.

Olapade OA, Leff LG. 2005. Seasonal response of stream biofilm communities to dissolved organic matter and nutrient enrichments. Appl Environ Microb 71:2278–2287.

Patrick R. 1969. Some effects of temperature on freshwater algae. In: Kendel PA, Parker FL, editors. Biological aspects of thermal pollution. Knoxville (TN): Vanderbilt University Press. p. 161–168.

Perkins KJ, Andrewartha JM, McMinn A, Cook SS, Hallegraeff GM. 2010. Succession and physiological health of freshwater microalgal fouling in a Tasmanian hydropower canal. Biofouling 26:637–644.

Rao TS. 2010. Comparative effect of temperature on biofilm formation in natural and modified marine environment. Aquat Ecol 44:463–478.

Ratkowsky DA, Olley J, Mcmeekin TA, Ball A. 1982. Relationship between temperature and growth rate of bacterial cultures. J Bacteriol 149:1–5.

Raven J, Geider R. 1988. Temperature and algal growth. New Phytol 110:441–461.

Rier ST, Stevenson RJ. 2002. Effects of light, dissolved organic carbon, and inorganic nutrients on the relationship between algae and heterotrophic bacteria in stream periphyton. Hydrobiologia 489:179–184.

Romaní AM. 2010. Freshwater biofilms. In: Dürr S, Thomason JC, editors. Biofouling. Oxford, UK: Wiley-Blackwell. p. 137–153.

Romaní AM, Sabater S. 1999. Effects of primary producers on the heterotrophic metabolism of a stream biofilm. Freshwater Biol 41:729–736.

Romaní AM, Fund K, Artigas J, Schwartz T, Sabater S, Obst U. 2008. Relevance of polymeric matrix enzymes during biofilm formation. Microb Ecol 56:427–436.

Romaní AM, Guasch H, Muñoz I, Ruana J, Vilalta E, Schwartz T, Emtiazi F, Sabater S. 2004. Biofilm structure and function and possible implications for riverine DOC dynamics. Microb Ecol 47:316–328.

Sabater S, Elosegi A, Acuña V, Basaguren A, Muñoz I, Pozo J. 2008. Effect of climate on the trophic structure of temperate forested streams. A comparison of Mediterranean and Atlantic streams. Sc Tot Environ 390:475–484.

Sander BC, Kalff J. 1993. Factors controlling bacterial production in marine and freshwater sediments. Microb Ecol 26:79–99.

Sand-Jensen K, Pedersen NL, Søndergaard M. 2007. Bacterial metabolism in small temperate streams under contemporary and future climates. Freshwater Biol 52:2340–2353.

Scott JT, Back JA, Taylor JM, King RS. 2008. Does nutrient enrichment decouple algal–bacterial production in periphyton? J N Am Benthol Soc 27:332–344.

Staehr PA, Sand-Jensen K. 2006. Seasonal changes in temperature and nutrient control of photosynthesis, respiration and growth of natural phytoplankton communities. Freshwater Biol 51:249–262.

Stoodley P, Wilson S, Hall-Stoodley L, Boyle JD, Lappin-Scott HM, Costerton JW. 2001. Growth and detachment of cell clusters from mature mixed-species biofilms. Appl Environ Microbiol 67:5608–5613.

Tresse O, Lescob S, Rho D. 2003. Dynamics of living and dead bacterial cells within a mixed-species biofilm during toluene degradation in a biotrickling filter. J Appl Microbiol 94:849–855.

Vasseur DA, McCann KS. 2005. A mechanistic approach for modeling temperature-dependent consumer-resource dynamics. Am Nat 166:184–198.

Ventura M, Liboriussen L, Lauridsen T, Søndergaard M, Søndergaard M, Jeppesen E. 2008. Effects of increased temperature and nutrient enrichment on the stoichiometry of primary producers and consumers in temperate shallow lakes. Freshwater Biol 53:1434–1452.

Weisse T, Stadler P, Lindström ES, Kimmance SA, Montagnes DJS. 2002. Interactive effect of temperature and food concentration on growth rate: a test case using the small freshwater ciliate *Urotricha farcta*. Limnol Oceanogr 47:1447–1455.

Wey JK, Scherwass A, Norf H, Arndt H, Weitere M. 2008. Effects of protozoan grazing within river biofilms under semi-natural conditions. Aquat Microb Ecol 52:283–296.

Xavier JB, Picioreanu C, van Loosdrecht MCM. 2005. A general description of detachment for multidimensional modelling of biofilms. Biotechnol Bioeng 91:651–669.

Ylla I, Borrego C, Romaní AM, Sabater S. 2009. Availability of glucose and light modulates the structure and function of a microbial biofilm. FEMS Microb Ecol 69:27–42.